J Mol Model (2013) 19:2423–2432
DOI 10.1007/s00894-013-1790-3

ORIGINAL PAPER

Acylglucuronide in alkaline conditions: migration vs. hydrolysis

Florent Di Meo · Michele Steel · Picard Nicolas · Pierre Marquet · Jean-Luc Duroux · Patrick Trouillas

Received: 10 October 2012 / Accepted: 1 February 2013 / Published online: 19 February 2013

Abstract This work rationalizes the glucuronidation process (one of the reactions of the phase II metabolism) for drugs having a carboxylic acid moiety. At this stage, acylglucuronides (AG) metabolites are produced, that have largely been reported in the literature for various drugs (*e.g.*, mycophenolic acid (MPA), diclofenac, ibuprofen, phenylacetic acids). The competition between migration and hydrolysis is rationalized by adequate quantum calculations, combing MP2 and density functional theory (DFT) methods. At the molecular scale, the former process is a real rotation of the drug around the glucuconic acid. This chemical-engine provides four different metabolites with various toxicities. Migration definitely appears feasible under alkaline conditions, making proton release from the OH groups. The latter reaction (hydrolysis) releases the free drug, so the competition is of crucial importance to tackle drug action and elimination. From the theoretical data, both migration and hydrolysis appear kinetically and thermodynamically favored, respectively.

Keywords Acylglucuronides · Alkaline hydrolysis · DFT · Kinetics · Migration · Thermodynamics

Electronic supplementary material The online version of this article (doi:10.1007/s00894-013-1790-3) contains supplementary material, which is available to authorized users.

F. Di Meo (✉) · M. Steel · J.-L. Duroux · P. Trouillas
School of Pharmacy, Université de Limoges,
2 rue du Docteur Marcland,
87025 Limoges Cedex, France
e-mail: florent.di-meo@unilim.fr

P. Nicolas · P. Marquet
Inserm, UMR-S850, 2 rue du Docteur Marcland,
87025 Limoges, France

P. Nicolas · P. Marquet
Laboratory of Medical Pharmacology, Université de Limoges,
2 rue du Docteur Marcland,
87025 Limoges, France

P. Nicolas · P. Marquet
Department of Pharmacology-Toxicology, CHU Limoges,
2 rue du Docteur Marcland,
87025 Limoges, France

P. Trouillas
Service de Chimie des Matériaux Nouveaux,
Université de Mons-Hainaut, 7000 Mons, Belgium

P. Trouillas
Regional Centre of Advanced Technologies and Materials,
Department of Physical Chemistry, Faculty of Science,
Palacký University Olomouc, tr. 17 listopadu,
771 46 Olomouc, Czech Republic

Introduction

Metabolism is a key event in human health, being responsible for the chemical transformation of xenobiotics in the body. The process can be divided into three main phases. The first phase (phase I) includes all the oxidative enzyme-catalyzed reactions. The second phase (phase II) consists of conjugation reactions (*e.g.*, glucuroconjugation, sulfoconjugation and methylation), which further increase xenobiotic hydrophilicity and helps transportability and elimination in urines of the conjugated compounds [1, 2]. The third phase consists of excretion of the drug metabolite. Drug metabolism can result in metabolites bearing different pharmacological properties from the parent drug. In the worst case scenario, these metabolites may be toxic. Phase II metabolism is crucial since it is a major determinant of the method of drug elimination, which indirectly influences the duration and intensity of the pharmacological effect.

In the present work we mainly focus on the glucuronidation process. A number of important drugs contain a carboxylic acid moiety for which glucuronidation is catalyzed by UDP-glucuronosyltransferases, which add glucuronic acid (**Glc-COOH**) on the OH group of the carboxylic moiety to produce

acylglucuronides (AG). These metabolites have largely been reported in the literature for various drugs (*e.g.*, mycophenolic acid (MPA) [3–6], diclofenac [7], ibuprofen [8], phenylacetic acids [9]). The presence of an ester bond confers AGs specific reactivity (*e.g.*, hydrolysis, nucleophilic attack) and pharmacological behavior.

Four possible AG isomers exist (*i.e.*, compounds **1**, **2**, **3** and **4** as defined in Scheme 1), according to the glucuronide O-atom involved in the ester bond. Isomerization from one to another is the so-called migration reaction process [9–11]. Differences in biological behavior have been observed between these different isomers. As an example compounds **3** and **4** have been suggested to form aldehyde intermediates, while the other two isomers do not [12, 13]. These reactive intermediates are known to covalently bind to proteins leading in some cases to immunoreactive proteins associated with drug hypersensitivity [14]. AGs have also been associated with serious liver toxicity, leading to the market withdrawal of some drugs [15].

The migration process can be depicted as the drug rotation around the glucuronic acid (Scheme 1). Two mechanisms have been proposed in the literature. The first one (M1) involves the formation of a stable five-membered ring intermediate (Scheme 2b) [8, 10]. The second (M2) is a base-catalyzed mechanism, which involves a charged five-membered intermediate (Scheme 2b) [16]. Both mechanisms are in agreement with some experimental studies that have demonstrated the presence of the five-membered ring intermediates.

However, AGs can also be hydrolyzed under alkaline conditions, which regenerate the free drug [9]. Hydrolysis is in competition with the migration mechanism (Scheme 1). The most common mechanism of alkaline hydrolysis is a B_{AC}^2 like reaction (base-catalyzed, bimolecular and acyl oxygen cleavage) [17–19]. It is a two-step reaction (Scheme 2a) characterized by the presence of a tetrahedral intermediate.

To the best of our knowledge, there exists only one theoretical study of glucuronidation processes, and it focuses solely on possible migration mechanisms [16]. By contrast, this paper aims to provide a detailed theoretical understanding of the factors which regulate glucuronidation and to rationalize the competition between hydrolysis and migration. Thermodynamics and kinetics of the possible mechanisms (migration and hydrolysis) were studied by using a combination of density functional theory (DFT) and post-Hartree-Fock (MP2) formalisms. A small AG prototype (acetoxyglucuronide acid, R=CH_3 in Schemes 1 & 2) was used to study the entire processes and extrapolation to larger compounds and numerous drugs is discussed in conclusion.

Calculation methodology

Both reactions hydrolysis and migration centre on an O-Csp^2 cleavage following an attack by a nucleophilic group, and so a simulation method which accurately describes this process must first be determined. All calculations were performed with the Gaussian03 program [20].

DFT is a well-established approach for investigating the thermodynamics of chemical reactions for middle size molecular systems. Numerous functionals have been developed to describe delocalized electronic structures, which are common in biomolecules, with increasing accuracy. DFT allows a much lower computational cost with respect to post-Hartree Fock (post HF) methods including MP2. Classical hybrid DFT functionals accurately describe thermodynamics for most of molecular systems. Concerning kinetics, they may provide well-defined geometries of transition states (TS) but the corresponding energies are known to be underestimated and non-unrealistic [21]. MP2 provides much better TS energies but dramatically increase the computational time, particularly when to calculate the corresponding geometries. A recent theoretical study [22] of the B_{AC}^2 reaction on small molecular prototypes (ethyl acetate) showed the relevance of MP2 energy calculations based on DFT geometries for such reactions. This joint DFT/MP2

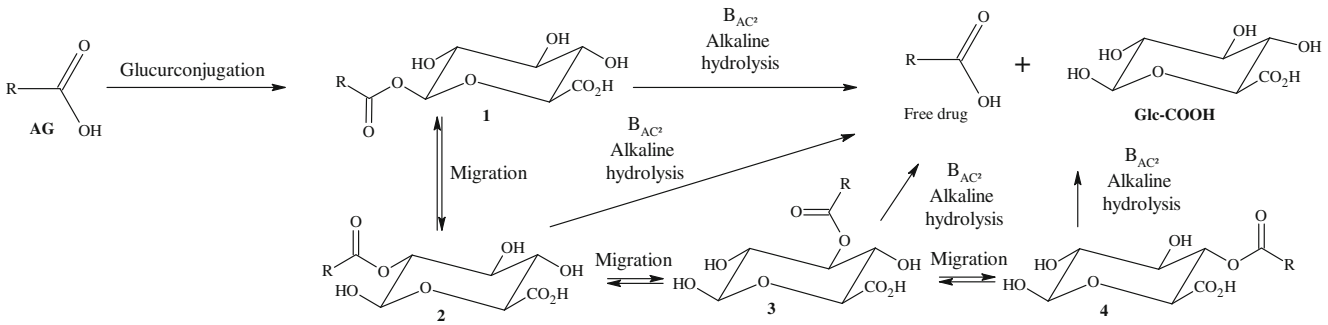

Scheme 1 Global scheme of AG reactivity (hydrolysis and migration). The four isomers quoted **1**, **2**, **3** and **4** correspond to 1-acetoxyglucuronide, 2-acetoxyglucuronide, 3-acetoxyglucuronide and 4-acetoxyglucuronide, respectively. It must be stressed that only compound 1 is formed by the enzymatic glucuronidation process

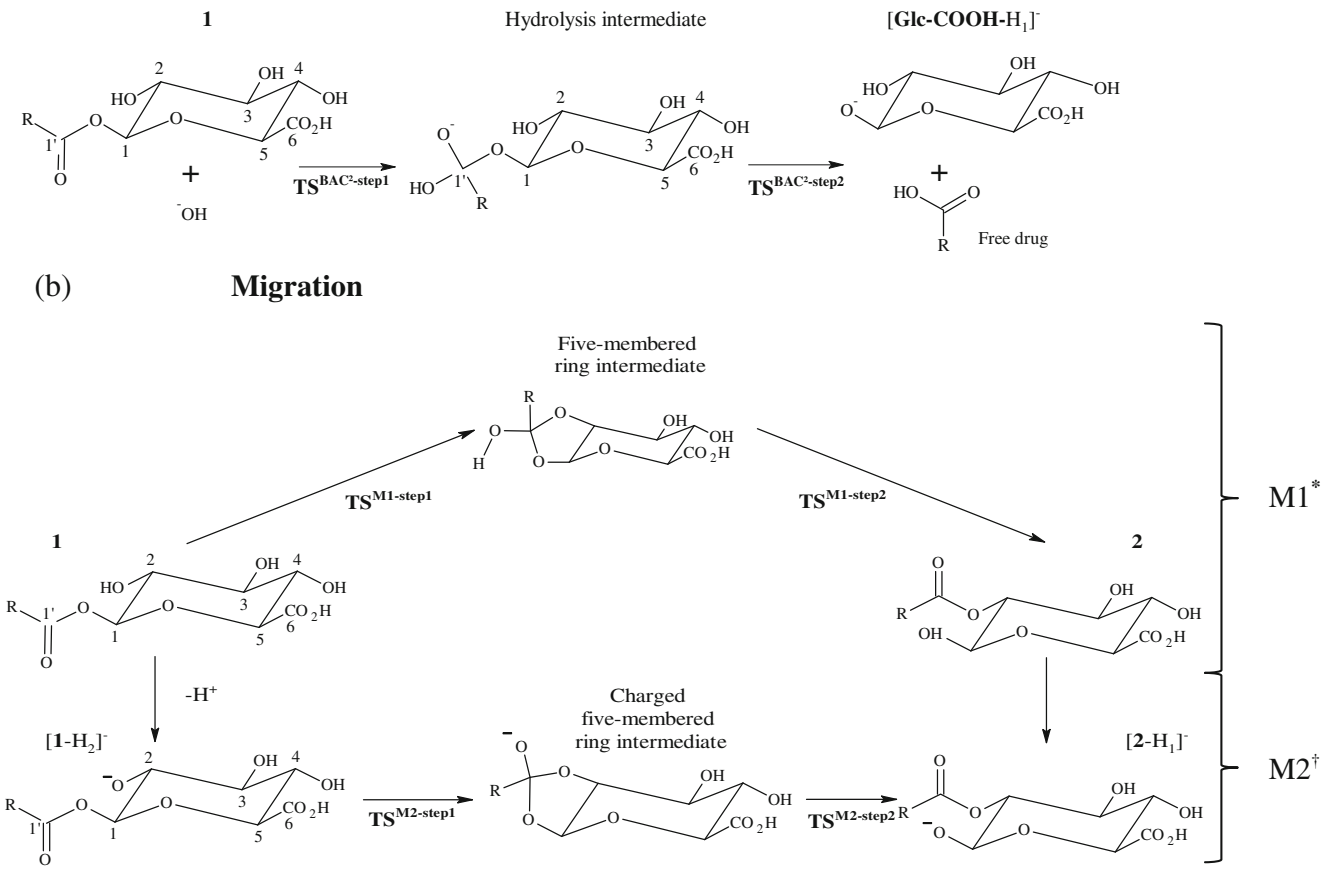

Scheme 2 Reaction pathways of alkaline hydrolysis (**a**) and migration (**b**) for compound 1. Configurations for hydrolysis products and transition states are illustrated in Fig. 1; while configurations for M1 and M2 migration transition states are illustrated in Figs. 2 and 3 respectively. * Transition states of M1 first and second steps are quoted $TS^{M1\text{-step1}}$ and $TS^{M1\text{-step1}}$, respectively. The second anionic of M2 are quoted [**2**-H_1]$^-$, [**3**-H_2]$^-$, or [**4**-H_3]$^-$, respectively. †In M2, anionic forms (after proton release from isomers **1**, **2** and **3**) are quoted [**1**-H_2]$^-$, [**2**-H_3]$^-$ and [**3**-H_4],$^-$ respectively

approach for geometries and energies, respectively has appeared as a relevant compromise between computational time and accuracy to rationalize the kinetics of the B_{AC}^2 reaction [22].

Geometry optimization, frequency analysis, zero point energy (ZPE) and thermal contributions to translation, rotation and vibration at 298 K were thus obtained at the B3P86/6-31g+(d,p)[1] level [23–25]. Electronic energies were calculated at the MP2/6-31++g(d,p) level [26, 27]. In order to confirm the agreement between this MP2/6-31g++(d,p) //B3P86/6-31g+(d,p) methodology and the experimental data, the kinetics was calculated for a prototype reaction (B_{AC}^2 hydrolysis of ethylacetate) similar to those studied in this work and for which experimental data are available:

$$CH_3 - COOC_2H_5 + OH^- \rightarrow CH3 - COO^- + H_2O.$$

In this case, the experimental activation barrier and theoretical free energy barrier were 11.0 and 10.5 kcal.mol^{-1}, respectively (Table 1). This prototype reaction was mainly related to hydrolysis, however since migration is also a O-Csp^2 bond cleavage, it appeared consistent to extrapolate the use of MP2/6-31g++(d,p)//B3P86/6-31g+(d,p) to the entire study. For computational tractability, the present work focuses on a simplified representative drug in which R=CH_3 (Schemes 1 and 2).

All stationary points were confirmed by the frequency analysis, *i.e.*, no imaginary frequency for stable geometries (reactants, intermediates and products) and one imaginary frequency for transition states, which was assigned to the

[1] The B3P86 functional is known to accurately evaluate bond dissociation enthalpies and so was used in this study to evaluate temperature-dependent corrections on the corresponding geometry.

Table 1 Energy barrier (kcal.mol^{-1}) of ethylacetate alkaline hydrolysis in water

	Energy barrier	Methods
Theor. ($\Delta G^{\#}$)	10.95	(IEFPCM) MP2/6-31g++(d,p)// B3P86/6-31g+(d,p)
Exp.	10.45	From ref. 22

vibration mode corresponding to the reaction coordinate under study (*i.e.* bond formation or cleavage). Transition states were also confirmed by the calculation of the minimum energy path using the integrated reaction coordinates (IRC) algorithm.

Solvent plays a determinant role in the studied mechanisms here. To use continuum models are the only feasible solution to study the whole mechanism since an explicit solvation would require account at least for the whole first solvation shell. Using explicit solvent would have required unfeasible computational effort since the number of degree of freedom would dramatically increase. Many implicit methods have been accurately used to model solvent effects for hydrolysis of small ester amides or other compounds [19, 22, 28]. In the present work, the implicit PCM (polarizable continuum model) formalism was used to model water in order to reproduce the physiological environment where these reactions take place. In implicit PCM, the molecular system is embedded in a shaped-adapted cavity surrounded by a homogenous dielectric medium, characterized by its dielectric constant. Integral equation formalism PCM (IEFPCM) [29–31]. The cavity surface was defined as overlapped spheres centered at each nucleus of heavy atoms, using UA0 radii. PCM is well-adapted to provide relative energies, which is adequate to achieve the aim of this work, *i.e.*, to study the competition between the different hydrolysis and migration reactions. The solvation free energies were corrected according to change in standard state conditions [32, 33].[2] This correction has an impact on A+B ->C reactions while due to compensation it has no effect on A+B -> C+D reactions.

Rate constants k are given according to the transition state theory (TST) by:

$$k_1 = \kappa(T)\frac{k_b T}{h}(C_0)^{-\Delta n}\exp\left(-\frac{\Delta G^{\#}}{RT}\right),$$

k_b is the Boltzmann's constant, T the temperature (298.15 K), h the Plank constant and R the ideal gas constant. $(C_0)^{-\Delta n}$ is equal to 1 because the calculated $\Delta G^{\#}$ (free energy activation barrier) was in molar standard conditions. The $\kappa(T)$ transmission coefficient (quantum tunneling along the reaction coordinate) was considered to be very close to 1 since tunneling may reasonably be considered negligible for a bond formation process involving two relatively big moieties. As tunneling was considered negligible, results will be mainly discussed in term of $\Delta G^{\#}$.

[2] This correction converts from standard state that uses a gas phase concentration of 1 atm and a liquid phase concentration of 1 mol.L^{-1} to free energies of solvation in the database which uses a standard state with a gas phase concentration of 1 mol.L^{-1} and a liquid phase concentration of 1 mol.L^{-1}, see refs [32] and [33].

Experimental details

The AG of mycophenolic acid (AG-MPA; a gift from Hoffmann–La Roche Ltd) was chosen as a model compound. A 1-g.L^{-1} stock solution was prepared in acetonitrile. AG-MPA was then diluted at 100 mg.L^{-1} in Hepes buffer (0.05 M; pH 7.4, pH 9 and pH 11) and incubated at 25°C over 48h. Aliquots (100 µl) were sampled at 0, 1h, 4h, 8h, 24h, and 48h and acidified with 15 µl of HCl (0.5 M). Samples were immediately frozen to avoid further degradation.

MPA and AG-MPA concentrations were then determined in each sample using a validated liquid chromatography tandem-mass spectrometry (LC-MS/MS) method previously described [3, 34].

Theoretical results and discussion

$B_{AC}2$ alkaline hydrolysis

The $B_{AC}2$ hydrolysis is a two-step mechanism. The first step is the nucleophilic attack by the hydroxide anion −OH. The second step is the C-O bond cleavage to form the carboxylic acid (free drug) and the deprotonated forms of glucuronic acid ([**Glc-COOH**-H_1]$^-$, [**Glc-COOH**-H_2]$^-$, [**Glc-COOH**-H_3]$^-$ and [**Glc-COOH**-H_4]$^-$, see Scheme 2a). The $B_{AC}2$ hydrolysis appears favorable, exhibiting $\Delta G°$ of −22.1, −14.3, −12.6 and −11.0 kcal.mol^{-1} for **1**, **2**, **3** and **4**, respectively (Table 2). All four hydrolysis products (Scheme 2a) are stabilized by the presence of one or two H bond(s) between the negative charged O-atom and the neighboring OH groups (Fig. 1a–d). This process is much favored for **1**

Table 2 Thermodynamics ($\Delta G°$, kcal.mol^{-1}), relative stabilities of intermediates with respect to the corresponding reactants (kcal.mol^{-1}), activation barriers of $B_{AC}2$-step2 ($\Delta G^{\#}$, kcal.mol^{-1}) and corresponding rate constants (k, M^{-1}.s^{-1})

	$\Delta G°$	Intermediate relative stability	$\Delta G^{\#}$	k
1-hydrolysis	−22.1	7.2	10.6	1.1×10^5
2-hydrolysis	−14.3	11.6	4.6	2.7×10^9
3-hydrolysis	−12.6	15.2	5.3	8.2×10^8
4-hydrolysis	−11.0	13.9	17.0	2.2

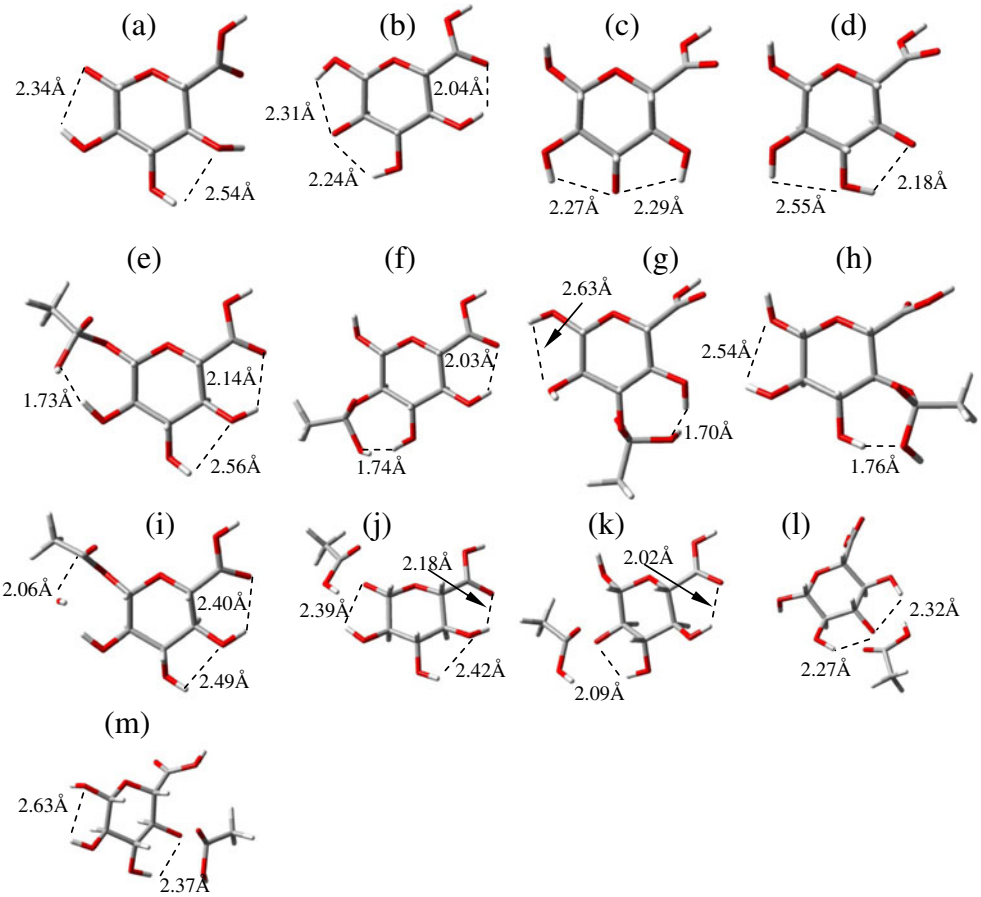

Fig. 1 3D conformations of hydrolysis products: [**Glc-COOH**-H_1]$^-$ (**a**), [**Glc-COOH**-H_2]$^-$ (**b**), [**Glc-COOH**-H_3]$^-$ (**c**), [**Glc-COOH**-H_4]$^-$ (**d**); hydrolysis intermediates **1**-hydrolysis (**e**), **2**-hydrolysis (**f**), **3**-hydrolysis (**g**) and **4**-hydrolysis (**h**); and transition states: $\mathbf{TS}^{\mathbf{BAC2\text{-}step1}}$ for **1**-hydrolysis (**i**) and $\mathbf{TS}^{\mathbf{BAC2\text{-}step2}}$ for **1**-hydrolysis (**j**), **2**-hydrolysis (**k**), **3**-hydrolysis (**l**) and **4**-hydrolysis (**m**). All predicted H bonds are shown

due to the better stability of [**Glc-COOH**-H_1]$^-$ with respect to [**Glc-COOH**-H_2]$^-$, [**Glc-COOH**-H_3]$^-$ and [**Glc-COOH**-H_4]$^-$ (Scheme 2a). This is mainly rationalized by the negative charge on the O-atom (alcoholate) that is −1.04 compared to −1.10, −1.09 and −1.08, respectively (Supplementary information), indicating a better charge delocalization and therefore a better stability for [**Glc-COOH**-H_1]$^-$.

The relative stability of the hydrolysis intermediates (Scheme 2a) with respect to the corresponding reactant is higher for the hydrolysis of **1** compared to **2**, **3** and **4** (Table 2). For **3**-hydrolysis the intermediate appears to be the least stabilized since in this case the H bond between the carboxylic group and the OH group at C_4 vanishes (Fig. 1e–h), decreasing the global stability of this intermediate by around 3 kcal.mol^{-1}.

The activation barrier of the first step is expected to be similar for the four attacks (*i.e.* on **1**, **2**, **3** and **4**, respectively). The transition state of the −OH attack on **1** is characterized by a distance of 2.06 Å between −OH and C_1 (Fig. 1i). The corresponding activation barrier and rate constant are 16.4 kcal.mol^{-1} and 5.27 $M^{-1}.s^{-1}$, respectively. This demonstrates that the first step of $B_{AC}2$ hydrolysis is relatively slow.

The second step appears relatively fast but dependent on intermediates, the activation barriers being 10.6, 4.6, 5.3 and 17.0 kcal.mol^{-1} (corresponding to rate constants of 1.1x10^5, 2.7x10^9, 8.2x10^8, and 2.2 $M^{-1}.s^{-1}$, respectively) (Table 2). The C-O bond cleavage (second step) is significantly slower for **1** than for **2** and **3** due to a better charge delocalization in the last two corresponding TS (charge on $O_{1'}$ is −0.986, −0.878 and −0.875 in $\mathbf{TS}^{\mathbf{BAC2\text{-}step2}}$ of **1**, **2** and **3**-hydrolysis, respectively). The kinetics is the slowest for the **4**-hydrolysis, for which the transition state is less stable mainly due to steric interaction between methyl and carboxylic groups and partially due to the lack of intra-molecular H bonding between the carboxylic group (Fig. 1m). The major role of H-bonding in this reaction is particularly emphasized in this step, during which a H bond is cleaved and a new one is formed between the negative O-atom and the neighboring OH group (2.39, 2.09, 2.27 and 2.37 Å for $\mathbf{TS}^{\mathbf{BAC2\text{-}step2}}$ of **1**, **2**, **3** and **4**-hydrolysis, respectively see Fig. 1i–m).[3] For example, the negative O-atom of the **1**-hydrolysis Step2-TS is stabilized by only one weak H bond (2.39 Å, Fig. 1j) vs. two for **3**-hydrolysis TS (2.27 and 2.32 Å, Fig. 1j and l), hence explaining the slower kinetics for **1**-hydrolysis.

[3] As can be seen in Supplementary information, the hydroxide negative charge is transferred during reaction (i.e., from reactants to TSs and then to products) from O1′ to the O-atom involved in the C-O cleavage (i.e., O1, O2, O3 and O4 in $TSB_{AC}2$-step2 of **1**, **2**, **3** and **4**-hydrolysis, respectively).

Migration

Mechanism M1 M1 is a two-step process (Scheme 2b). Both steps are similar from a chemical point of view, being driven by C-O bond cleavages coupled with proton transfer. M1 is a thermodynamically favorable event but exhibiting relatively low ΔG values −4.5, −0.4 and −2.0 kcal.mol^{-1} for **1**->**2**, **2**->**3** and **3**->**4** transitions, respectively (Table 3a). The relative stabilities of **2**, **3** and **4** with respect to **1** are −4.5, -4.9 and −6.9 kcal.mol^{-1}, respectively (Table 3).

All five-membered ring intermediates of the M1 process (Scheme 2b) are less stable than their corresponding products (**2**, **3** and **4**), by more than 10 kcal.mol^{-1} (Table 3a). This instability mainly stems from the strong constraint that occurred in the equatorial dioxo-ring. The conformation of this ring is very similar for the three intermediates, thus leading to very similar relative energies with respect to the reactant (Table 3a).

The activation barriers of the first step, from the reactant to the five-membered ring intermediates, are 56.5, 62.8 and 57.2 kcal.mol^{-1} for **1**->**2**, **2**->**3** and **3**->**4**, respectively (Table 3a). The first step of **2**->**3** is slower than for **1**->**2** and **3**->**4** due to a less efficient charge repartition in the corresponding TS (charges on O_2, O_3 and O_4, *i.e.*, O-atom that attacks the C=O group, are −0.756, −0.929 and −0.759 for $\mathbf{TS}^{\mathbf{M1\text{-}step1}}$ of **1**->**2**, **2**->**3** and **3**->**4**, respectively, see Supplementary information). The C-O bond distances that correspond to the five-membered ring formation in these TSs are 1.8, 2.1 and 1.8 Å, respectively (Fig. 2a–c) and the dipole moment of the corresponding bond are 2.01 D, 1.89 D and 2.50 D, respectively, which confirms (i) the increased distortion of the five-membered ring in **2**->**3**-TS and (ii) the decrease of anionic O-atom stabilization, making it less stable.

The M1 second step is the coupled-proton-transfer C-O bond cleavage of the five-membered ring intermediates leading to **2**, **3** and **4**. The corresponding activation barriers are 38.1, 52.1 and 49.1 kcal.mol^{-1}, respectively, which correspond to rate constants of 10^{-16}, 10^{-26} and 10^{-24} $M^{-1}.s^{-1}$, respectively. This step is fastest for **1**->**2** due to the presence of two stabilizing H bonds in the corresponding TS (Fig. 2d), whereas the other two TSs (*i.e.*, **2**->**3** and **3**->**4**) have only one H bonds (Fig. 2e and f).

Mechanism M2 M2 can only occur under alkaline conditions, making proton release from the OH groups of AGs feasible. Deprotonation from **1**, **2** and **3** leads to the deprotonated intermediates [**1**-H_2]$^-$, [**2**-H_3]$^-$ and [**3**-H_4]$^-$ (Scheme 2b). This step favors the formation of charged five-membered ring intermediates and the subsequent C-O bond cleavage to form [**2**-H_1]$^-$, [**3**-H_2]$^-$ and [**4**-H_3]$^-$ (Scheme 2b). Disregarding de-protonation and re-protonation, M2 is a two-step mechanism (Scheme 2b), the negative charge being transferred from one to another O-atom (*e.g.*, charges on O_1, O_2 and $O_{1'}$ are [−0.55, −1.15 and −0.75], [−0.74, −0.66 and −1.01] and [−1.05, −0.61 and −0.76] in [**1**-H_2]$^-$, the intermediate and [**2**-H_1]$^-$, respectively, see in Supplementary information).

From the deprotonated forms, the [**1**-H_2]$^-$->[**2**-H_1]$^-$ migration is thermodynamically favorable (ΔG°=−13.8 kcal.mol^{-1}) while the [**2**-H_3]$^-$->[**3**-H_2]$^-$ and [**3**-H_4]$^-$->[**4**-H_3]$^-$ are unfavorable (ΔG°=+7.9 and +10.5 kcal.mol^{-1}, respectively) (Table 3b). This shows that [**2**-H_1]$^-$ is the most stable deprotonated-isomer. This better stability is attributed to a better charge delocalization in the hemiacetal moiety (*e.g.*, charges on the anionic O-atom are −1.053, −1.057 and −1.117 in [**2**-H_1]$^-$, [**3**-H_2]$^-$ and [**4**-H_3]$^-$, respectively). All the charged five-membered ring intermediates are less stable than their corresponding reactants by 3.9, 7.2 and 8.0 kcal.mol^{-1} (Table 3b).

The activation barriers of the M2 first step (Scheme 2b) are 5.8, 12.0 and 9.6 kcal.mol^{-1} (k=10^8, 10^4 and 10^5 $M^{-1}.s^{-1}$, Table 3b) for [**1**-H_2]$^-$->[**2**-H_1]$^-$, [**2**-H_3]$^-$->[**3**-H_2]$^-$ and [**3**-H_4]$^-$->[**4**-H_3]$^-$, respectively. This step is fastest for the first process due to the low stability of [**1**-H_2]$^-$ reactant over its product, as compared to the [**2**-H_3]$^-$ and [**3**-H_4]$^-$ reactants (Table 4).

Table 3 Thermodynamics (ΔG°, kcal. mol^{-1}), relative stabilities of five-membered ring intermediates with respect to the corresponding isomer (kcal.mol^{-1}), activation barriers ($\Delta G^{\#}$, kcal.mol^{-1}) and corresponding rate constants (k, $M^{-1}.s^{-1}$) of (a) M1 and (b) M2 migration

	ΔG°	Intermediate relative stability	$\Delta G^{\#step1}$	k^{step1}	$\Delta G^{\#step2}$	k^{step2}
(a)						
1->**2**	−4.5	10.8	56.5	2.8×10^{-29}	38.1	7.6×10^{-16}
2->**3**	−0.4	13.7	62.8	6.4×10^{-34}	52.1	4.2×10^{-26}
3->**4**	−2.0	13.1	57.2	7.8×10^{-30}	49.1	6.4×10^{-24}
(b)						
[**1**-H_2]$^-$->[**2**-H_1]$^-$	−13.8	3.9	5.8	3.6×10^{8}	2.2	1.5×10^{11}
[**2**-H_3]$^-$->[**3**-H_2]$^-$	7.9	7.2	12.0	9.8×10^{3}	3.6	1.5×10^{10}
[**3**-H_4]$^-$->[**4**-H_3]$^-$	10.5	8.0	9.6	5.7×10^{5}	9.7	5.1×10^{5}

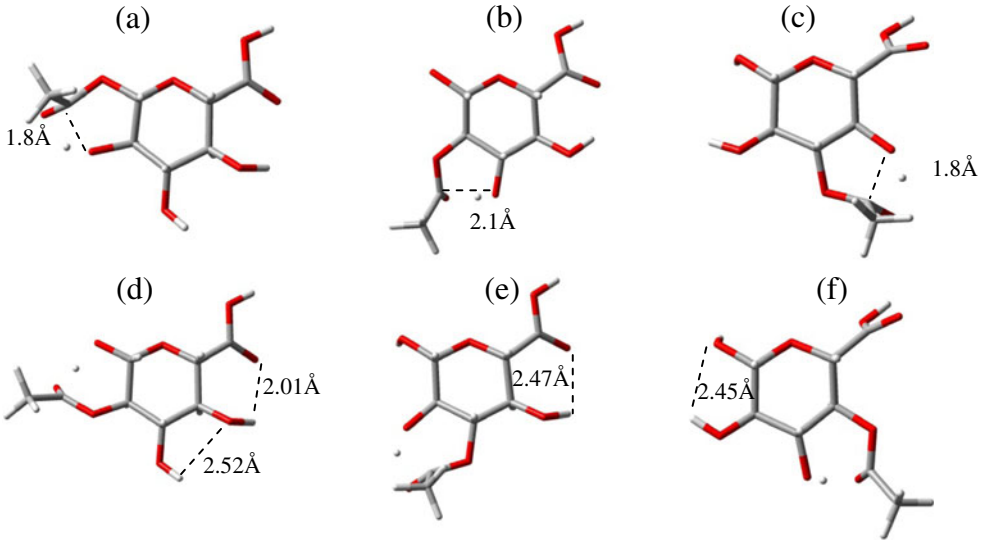

Fig. 2 3D conformations of $\mathbf{TS}^{\mathbf{M1\text{-}step1}}$ of **1**->**2** (**a**), **2**->**3** (**b**), **3**->**4** (**c**) exhibiting C-O bond distances corresponding to the five-membered ring formation and $\mathbf{TS}^{\mathbf{M1\text{-}step2}}$ for reaction of **1**->**2** (**d**), **2**->**3** (**e**), **3**->**4** (**f**) exhibiting stabilizing H-bonds

The M2 second step is the C-O bond cleavage (Scheme 2b) from each intermediate to form the corresponding deprotonated products ($[\mathbf{2}\text{-}H_1]^-$, $[\mathbf{3}\text{-}H_2]^-$ and $[\mathbf{4}\text{-}H_3]^-$). The activation barriers are significantly lower than for the first step, except for the third process (2.2, 3.6 and 9.7 kcal.mol^{-1}, respectively) (Table 3b). The relatively low rate constant of the third mechanism is mainly attributed to the instability of the corresponding $\mathbf{TS}^{\mathbf{M2\text{-}step2}}$, which is primarily due to the absence of strong H-bonds and less delocalized charge (Fig. 3). The first step (*i.e.*, five-membered ring formation) hence appears as the limiting step of M2, but this migration pathway is kinetically favored over M1.

Conclusions-MPA degradation

The above reported theoretical simulations have indicated that M2 migration is kinetically favored over M1, and that it is faster than the hydrolysis. We have thus confirmed a viable pathway for drug metabolization by glucuronidation, all be it one that can only take place under alkaline conditions. The different isomers yielded by migration are kinetic products while drug release by hydrolysis is the thermodynamic product. These conclusions can be easily extended to the large series of drugs having the carboxylic moiety.

A "direct" migration pathway avoiding any intermediate has also been suggested. However it does not fit with experimental data reporting on the presence of five-membered ring intermediates [10]. Another proof in favor of M2 is that this mechanism is allowed only under alkaline conditions, which is in very good agreement with experimental evidences. Experiments to measure the rate of drug metabolization by glucuronidation were performed using MPA. This drug was chosen because (i) it is widely used in the medical area, and greater insight into its behavior in the body is important (ii) it has already been the subject of other theoretical/experimental studies, so there is a large volume of knowledge to corroborate our theory.

MPA (Fig. 4) is a typical drug providing AG derivatives. Therefore the degradation of AG-MPA (Fig. 4) under physiological pH conditions is very characteristic. Its stability over 48 h is limited and dramatically influenced by the pH. At pH 7.4, AG-MPA concentrations remained stable up to 4 h and then decreased steadily to reach 41% of the initial quantity incubated (Fig. 4a). At pH 9, AG-MPA degradation was much more pronounced: 50% of the initial quantity incubated disappeared after 1 h and 5% remained after 48 h (Fig. 4a). No residual AG-MPA could be detected in any of the samples of the incubation conducted at pH 11, suggesting an immediate and complete degradation of the acyl-glucuronide.

Table 4 Relative free energies (ΔG, kcal.mol^{-1}) of all reactants and products with respect to the initial deprotonated ($[\mathbf{1}\text{-}H_2]^-$) for M2 migration pathways

Compound	$[\mathbf{1}\text{-}H_2]^-$	$[\mathbf{2}\text{-}H_1]^-$	$[\mathbf{2}\text{-}H_3]^-$	$[\mathbf{3}\text{-}H_2]^-$	$[\mathbf{3}\text{-}H_4]^-$	$[\mathbf{4}\text{-}H_3]^-$
ΔG	0.0	−13.8	−6.1	1.8	−7.8	2.7

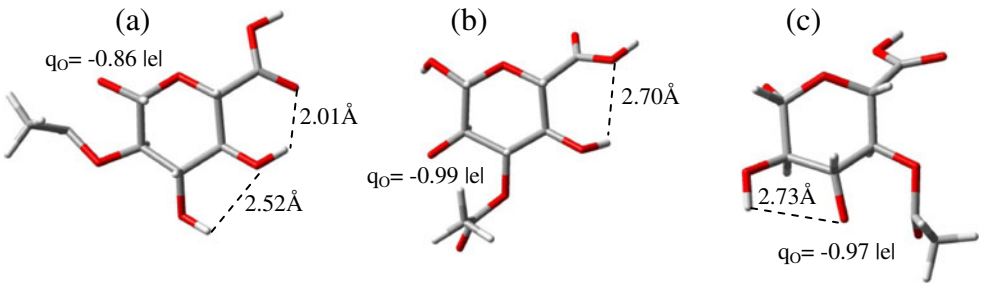

Fig. 3 3D conformations of $TS^{M2\text{-}step2}$ of **1**->**2** (**a**), **2**->**3** (**b**), **3**->**4** (**c**) exhibiting C-O bond distances between the O^- and the $C_{1'}$ atoms, predicted H-bonds and anionic O-atom partial

MPA resulting from the degradation of AG-MPA was monitored. As a consequence of the pH-dependence of AG-MPA degradation, MPA was formed in higher concentration at high pH (Fig. 4b). However, the quantity of MPA produced after 48 h was less than 10% of the quantity of AG-MPA which has disappeared. So even if

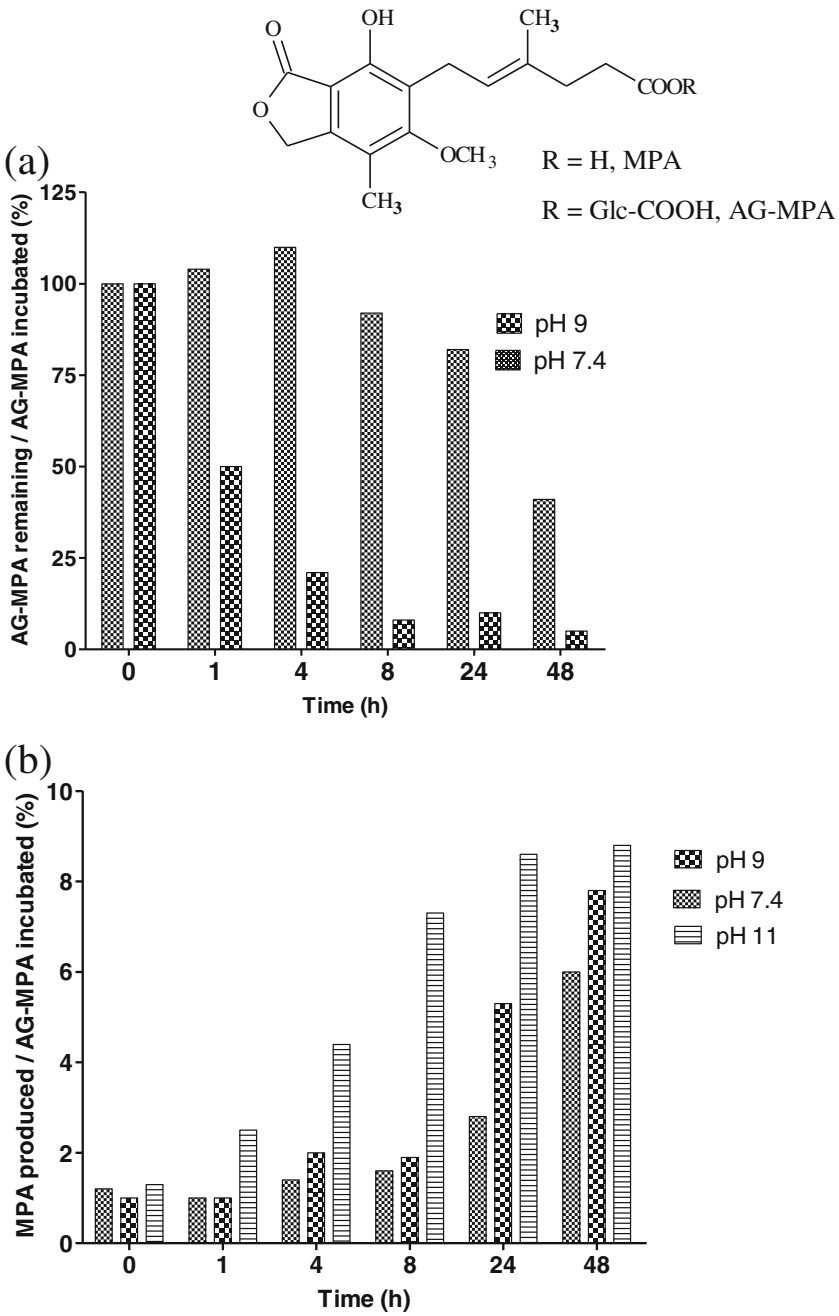

Fig. 4 Degradation of mycophenolic acid acyl-glucuronide (AG-MPA; upper panel) and the corresponding formation of MPA (bottom panel) as related to the initial quantity of AG-MPA incubated in HEPES buffer pH 7.4, 9 and 11

thermodynamically favorable, under physiological conditions alkaline hydrolysis appears not to be the only mechanism for AG (*e.g.*, AG-MPA) degradation. Migration is an alternative process. Nonetheless the M1 pathway is very slow and unlikely ($\Delta G^{\#}$ higher than 38 kcal.mol^{-1} and k lower than 8×10^{-16} $M^{-1}.s^{-1}$), especially under a physiological environment where numerous side reactions may occur. The M2 pathway thus appeared as the only chemical solution for migration. Under alkaline conditions, M2 is highly kinetically favored, making this process competitive with respect to alkaline hydrolysis.

As an extension of this highlighting work rationalizing migration vs. hydrolysis for the very important acyglucuronide metabolites, the use of an explicit first solvation shell is a future and motivating challenge. This would provide the exact role of intermolecular H-bonding in these processes. Also other environmental conditions could be of importance including the presence of metabolic enzymes.

Acknowledgments The authors thank the "Conseil Régional du Limousin" for financial support and CALI (CAlcul en LImousin) for computing facilities. The authors also gratefully acknowledge the support by COST (COST Action CM0804 "Chemical Biology with Natural Compounds") and the Operational Program Research and Development for Innovations–European Regional Development Fund (project CZ.1.05/2.1.00/03.0058 of the Ministry of Education, Youth and Sports of the Czech Republic).

References

1. Kaspersen FM, Van Boeckel CAA (1987) A review of the methods of chemical synthesis of sulphate and glucuronide conjugates. Xenobiotica 17:1451–1471
2. Stachulski AV, Jenkins GN (1998) The synthesis of O-glucuronides. Nat Prod Rep 15:173–186
3. Picard N et al (2005) Identification of the UDP-glucuronosyltransferase isoforms involved in mycophenolic acid phase II metabolism. Drug Metab Dispos 33:139–146
4. Schutz E et al (1999) Identification of a pharmacologically active metabolite of mycophenolic acid in plasma of transplant recipients treated with mycophenolate mofetil. Clin Chem (Washington, D C) 45:419–422
5. Shipkova M et al (1999) Identification of glucoside and carboxyl-linked glucuronide conjugates of mycophenolic acid in plasma of transplant recipients treated with mycophenolate mofetil. Br J Pharmacol 126:1075–1082
6. Shipkova M et al (2000) Determination of the acyl glucuronide metabolite of mycophenolic acid in human plasma by HPLC and Emit. Clin Chem (Washington, D C) 46:365–372
7. Grillo MP et al (2003) Studies on the chemical reactivity of diclofenac acyl glucuronide with glutathione: Identification of diclofenac-S-acyl-glutathione in rat bile. Drug Metab Dispos 31:1327–1336
8. Johnson CH et al (2007) NMR spectroscopic studies on the in vitro acyl glucuronide migration kinetics of ibuprofen ((Â±)-(R,S)-2-(4-Isobutylphenyl) propanoic acid), its metabolites, and analogues. Anal Chem (Washington, DC, United States) 79:8720–8727
9. Vanderhoeven SJ et al (2004) NMR and QSAR studies on the transacylation reactivity of model 1î^2-O-acyl glucuronides. I: Design, synthesis and degradation rate measurement. Xenobiotica 34:73–85
10. Corcoran O et al (2001) HPLC/1H NMR spectroscopic studies of the reactive Î±–1-O-acyl isomer formed during acyl migration of S-naproxen î^2-1-O-acyl glucuronide. Chem Res Toxicol 14:1363–1370
11. Hansen-Moeller J et al (1988) Isolation and identification of the rearrangement products of diflunisal 1-O-acyl glucuronide. J Pharm Biomed Anal 6:229–240
12. Spahn-Langguth H, Benet LZ (1992) Acyl glucuronides revisited: is the glucuronidation process a toxification as well as a detoxification mechanism? Drug Metab Rev 24:5–47
13. Wang J et al (2004) A novel approach for predicting acyl glucuronide reactivity via Schiff base formation: development of rapidly formed peptide adducts for LC/MS/MS measurements. Chem Res Toxicol 17:1206–1216
14. Park BK, Coleman JW, Kitteringham NR (1987) Drug disposition and drug hypersensitivity. Biochem Pharmacol 36:581–590
15. Boelsterli UA, Zimmerman HJ, Kretz-Rommel A (1995) Idiosyncratic liver toxicity of nonsteroidal antiinflammatory drugs: molecular mechanisms and pathology. Crit Rev Toxicol 25:207–235
16. Berry NG et al (2009) Synthesis, transacylation kinetics and computational chemistry of a set of arylacetic acid 1[small beta]-O-acyl glucuronides. Org Biorgan Chem 7:2525–2533
17. Bender ML (1960) Mechanisms of catalysis of nucleophilic reactions of carboxylic acid derivatives. Chem Rev (Washington, DC, United States) 60:53–113
18. Garcias RC et al (2003) Theoretical study of the alkaline hydrolysis of an aza-î^2-lactam derivative of clavulanic acid. Chem Phys Lett 372:275–281
19. Xiong Y, Zhan C-G (2004) Reaction pathways and free energy barriers for alkaline hydrolysis of insecticide 2-trimethylammonioethyl methylphosphonofluoridate and related organophosphorus compounds: electrostatic and steric effects. J Org Chem 69:8451–8458
20. Frisch MJ et al (2004) Gaussian 03, Revision C.02, edn. I. Gaussian 2004, Wallingford, CT
21. Zhao Y, Truhlar DG (2004) Hybrid meta density functional theory methods for thermochemistry, thermochemical kinetics, and noncovalent interactions: the MPW1B95 and MPWB1K models and comparative assessments for hydrogen bonding and van der Waals interactions. J Phys Chem A 108:6908–6918
22. Zhan C-G, Landry DW, Ornstein RL (2000) Energy barriers for alkaline hydrolysis of carboxylic acid esters in aqueous solution by reaction field calculations. J Phys Chem A 104:7672–7678
23. Trouillas P et al (2004) A theoretical study of the conformational behavior and electronic structure of taxifolin correlated with the free radical-scavenging activity. Food Chem 88:571–582
24. Trouillas P et al (2006) A DFT study of the reactivity of OH groups in quercetin and taxifolin antioxidants: the specificity of the 3-OH site. Food Chem 97:679–688
25. Anouar E et al (2009) New aspects of the antioxidant properties of phenolic acids: a combined theoretical and experimental approach. Phys Chem Chem Phys 11:7659–7668
26. Moller C, Plesset MS (1934) Note on the approximation treatment for many-electron systems. Phys Rev 46:618–622
27. Grimme S (2003) Improved second-order M[o-slash]ller–Plesset perturbation theory by separate scaling of parallel- and antiparallel-spin pair correlation energies. J Chem Phys 118:9095–9102
28. Pliego JR Jr, Riveros JM (2002) A theoretical analysis of the free-energy profile of the different pathways in the alkaline

hydrolysis of methyl formate in aqueous solution. Chem Eur J 8:1945–1953
29. Vilkas MJ, Zhan C-G (2008) An efficient implementation for determining volume polarization in self-consistent reaction field theory. J Chem Phys 129:194109/194101–194109/194107
30. Cossi M et al (2002) New developments in the polarizable continuum model for quantum mechanical and classical calculations on molecules in solution. J Chem Phys 117:43–54
31. Tomasi J, Mennucci B, Cammi R (2005) Quantum mechanical continuum solvation models. Chem Rev (Washington, DC, United States) 105:2999–3093
32. Abraham MH (1984) Thermodynamics of solution of homologous series of solutes in water. J Chem Soc Faraday Trans 1 Phys Chem Condens Phase 80:153–181
33. Jang YH et al (2002) pKa values of guanine in water: density functional theory calculations combined with Poisson−Boltzmann Continuum−Solvation Model. J Phys Chem B 107:344–357
34. Premaud A et al (2006) Determination of mycophenolic acid plasma levels in renal transplant recipients co-administered sirolimus: comparison of an enzyme multiplied immunoassay technique (EMIT) and liquid chromatography-tandem mass spectrometry. Ther Drug Monit 28:274–277